Changes in mobility of chromaffin granules in actin network with its assembly and Ca^{2+}-dependent disassemby by gelsolin

S. Miyamoto,* T. Funatsu,‡ S. Ishiwata,‡ and S. Fujime§

*Department of Biochemical Engineering, Faculty of Computer and Systems Engineering, Kyushu Institute of Technology, 680-4 Kawatsu, Iizuka, Fukuoka 820; ‡Department of Physics, School of Science and Engineering, Waseda University, 3-4-1 Okubo, Shinjuku, Tokyo 169; and §Graduate School of Integrated Science, Yokohama City University, 22-2 Seto, Kanazawa, Yokohama 236, Japan.

ABSTRACT As a final stage of cell signal transduction, secretory cells release hormones by exocytosis. Before secretory granules contact with the cell membrane for fusion, an actin-network barrier must dissociate as a prelude. To elucidate dynamical behaviors of secretory granules in actin networks, in vitro assembly and disassembly processes of actin networks were examined by means of dynamic light-scattering spectroscopy. We studied actin polymerization in the presence of chromaffin granules isolated from bovine adrenal medullas and found that the entanglement of actin filaments rapidly formed cages that confined granules in them. We also studied the effect of gelsolin, one of actin-severing proteins, on the network of actin filaments preformed in the presence of chromaffin granules. It turned out that the cages that confined granules rapidly disappeared when gelsolin was added in the presence of free Ca^{2+} ions. A semiquantitative analysis of dynamic light-scattering spectra permitted us to estimate the changes in the mobility (or the translational diffusion coefficient) of chromaffin granules in the actin network with its assembly and Ca^{2+}-dependent disassembly by gelsolin. Based on the present results and some pieces of evidence in the literature, a model is proposed for biophysical situations before, during, and after an exocytotic event.

INTRODUCTION

Many morphological investigations have shown that the cytoplasm of mammalian cells is highly organized and compartmentalized by the cytoskeleton. This organization and compartmentalization takes an important part in many processes of signal transduction, such as release of neuronal transmitters and secretion of hormones and enzymes. A cell receives external chemical signals by receptor molecules or electrical stimuli by channels in the membrane. Various molecular processes for transducing signals are activated by second messengers in the cytoplasm. As a final step, the cell releases the hormones or neurotransmitters by an exocytotic event. In secretory cells and neuronal synapses, hormones and neurotransmitters are stored, respectively, in secretory granules and synaptic vesicles. These granules and vesicles must contact with the cell membrane and fuse with it before release of their contents.

At a resting state, these granules are tightly or loosely held in dense cytoskeleton networks. Morphological and immunological investigations have shown that the dense network is made up of actin filaments, e.g., in the peripheral region of chromaffin cells and in the presynaptic nerve terminals (1–5). The actin network is considered to hold chromaffin granules in at least three ways, (Fig. 1): (*a*) actin filaments extending directly from α-actinin molecules on the granule membrane can form actin networks (6), (*b*) actin filaments connect granules to networks with a linkage molecule such as fodrin-like molecules (7–9), and (*c*) the network confines granules in a restricted space (a cage model). In a cytosolic situation, chromaffin granules would be trapped in combination of these possibilities and of equivalent ones. Our point is that only the liberation of cross-linker molecules from the network is not enough to mobilize the granules, because the movements of granules are still restricted in the dense network of actin filaments. In any case, the actin network must disassemble for granules to access the cell membrane as a prelude of exocytosis (2). Many actin-severing proteins have been identified in the cytoplasm of chromaffin cells (10–13). Severing functions of these proteins are activated by free Ca^{2+} ions in a micromolar level (14–18). In secretory and neuronal cells, the concentration of free Ca^{2+} ions in the cytosol, after receiving an external stimulus, increases to a micromolar level by releasing them from a carciosome and an influx through Ca^{2+} channels in the cell membrane (19, 20). In chromaffin cell cytosol and neuronal synaptic terminal, morphological and immunological investigations have confirmed, in the cortical region of the cell membrane, the existence of gelsolin (21, 22) and scinderin (18).

At present, it is technically difficult to observe the assembly and disassembly processes of the actin network in intact cell cytosol. In this study, therefore, we used an in vitro cell-free system to analyze dynamical processes of the network formation holding secretory granules and of the network dissociation by an actin-severing protein, gelsolin, in the presence of free Ca^{2+} ions. We used a dynamic light-scattering method (DLS) that is one of the most appropriate techniques to analyze a dynamical behavior of particles with submicrometer sizes in solution (23–25). So far, a falling ball method for viscosity measurements has been used to observe the formation and dissociation of actin filaments (7). This method,

This article is dedicated to Professor Sho Asakura, who is one of the pioneers of the study on actin polymerization, on the occasion of his retirement from Nagoya University (1991).

Please address all correspondence to S. Fujime.

0006-3495/93/04/1139/11 $2.00

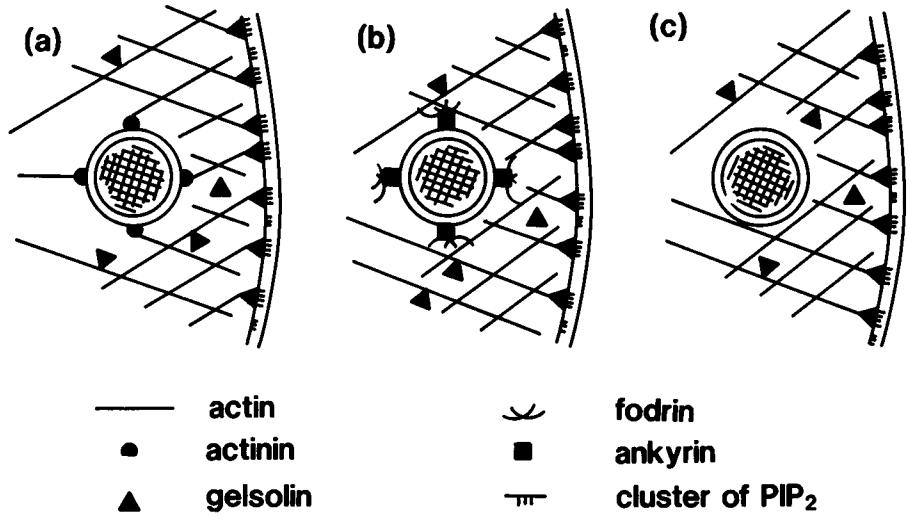

FIGURE 1 Schematic illustration of three model situations holding granules in the network of actin filaments in a resting cell (for details, see text).

however, may have a defect to cause a mechanical damage to the network/granules system. The DLS method makes it possible to detect the dynamical behavior of the granules and filaments without applying any mechanical perturbation. As a quick and intuitive method, however, viscometry was also used for some additional measurements.

Works related to the present study have been reported by Newman et al. (26, 27). They used polystylene latex spheres (PLS) instead of chromaffin granules in this study. They observed the change in mobility of PLS with formation of actin network (26). They also studied the mobility of PLS in solutions of F-actin, whose average length was varied by polymerization of actin in the presence of various amounts of gelsolin (27). In their studies, they set a condition that the scattering intensity from PLS was much higher than that from F-actin, so that they "saw" only the motion of PLS. In our system, which mimicked the cytosolic situation more closely than their system, the scattering intensity from granules was only several times higher than that from F-actin, so that we had to develop methods (given in the Appendixes) for estimation of mobility of chramaffin granules in F-actin network.

MATERIALS AND METHODS

Preparation of chromaffin granules

Bovine adrenal glands were obtained from a local slaughter house. After removing adipose tissue, the adrenal glands were extensively perfused to remove blood vessels perfectly at 37°C for 30 min with Ca^{2+}-free Krebs ringer solution (153 mM NaCl, 5.6 mM KCl, 3.6 mM $NaHCO_3$, 5 mM glucose, and 5 mM *N*-2-hydroxyethylpiperazine-*N'*-2-ethane sulfonic acid [Hepes] pH 7.0). The adrenal medullas were dissected to be free of cortical material and placed in 10 vol of an isotonic solution (300 mM sucrose, 10 mM Hepes, pH 7.0, 1 mM phenylmethylsulfonyl fluoride [PMSF], 1 mM dithiothreitol, 0.5 mM NaN_3, and 1 μg/ml leupeptin). The tissue was blended for 5 s in a blender (Waring Products Div., Dynamics Corp. of America, New Hartfort, CT), homogenized in a cylindrical glass homogenizer with a loose-fitting motor-driven Teflon pestle (Ikemoto Rika Co. Ltd., Tokyo, Japan), and filtered through four layers of gauze. The homogenate was centrifuged at 500 *g* for 5 min to remove unbroken cells and nuclei. The supernatant was centrifuged at 20,000 *g* for 30 min to pellet chromaffin granules. After discarding the supernatant, the isotonic solution was gently overlayed along the tube wall. The tube was carefully swirled to remove the upper fluffy layer of mitochondria on the pellet. The supernatant was carefully discarded without disturbing the pellet. The remainder of the pellet was gently resuspended in the same isotonic solution by hand homogenization in a glass/glass Ten Broek homogenizer (Wheaton Scientific Co. Ltd., Millville, NJ). The suspension was centrifuged at 10,000 *g* for 30 min. After the supernatant was discarded, the brown fluffy layer was dislodged by a gentle swirling as above. After the pellet was gently resuspended by hand homogenization, the suspension was centrifuged at 7,000 *g* for 30 min. After removing the fluffy layer, the pellet was resuspended in the isotonic solution. The discontinuous gradient was made by overlaying 3 ml of this suspension on 7 ml of 1.6 M sucrose solution in the centrifugation tube and centrifuged at 80,000 *g* for 60 min. The whitish-pink pellet (chromaffin granules) was resuspended in the isotonic solution and stored at 4°C. In this study, we used chromaffin granules within 48 h after their preparation.

Preparation of G-actin

G-actin from rabbit back and leg white muscle was prepared and purified by standard methods (28–30) with slight modifications. No column chromatography step was made. In the final step of purification, F-actin was dialyzed for 72 h against 0.1 mM Mg adenosine triphosphate (ATP) and 2 mM tris(hydroxymethyl)-aminomethane-HCl at pH 8.0.

Preparation of gelsolin

Gelsolin from calf plasma was prepared and purified by the method described elsewhere and stored in liquid nitrogen. In this light-scattering study, the gelsolin preparation used was from the same lot as in Funatsu et al. (31), where it was shown that the axial rigor stiffness of a chemically skinned muscle fiber, for example, decreased by 50% of the original size within 10 min after the fiber was bathed in Ca rigor solution containing 0.5 mg/ml gelsolin. The molecular weight of gelsolin was assumed to be 93 kD (32).

Polymerization of actin

Unless otherwise stated, solutions of 1 mg/ml G-actin (±0.5 mg/ml chromaffin granules) in 300 mM sucrose, 10 mM 3-(*N*-morpholino)propanesulfonic acid (MOPS), pH 7.0, 0.1 mM MgATP, 0.1 mM PMSF, and no (pCa > 7) or 10 μM free Ca^{2+} ions (pCa = 5) were prepared in light-scattering cells. The pCa values were determined by a multiequilibrium formulation, where the ethyleneglycol-bis(β-aminoethyl ether)-*N,N'*-tetraacetic acid-calcium binding constant in our condition was assumed to be $10^{5.5}$. Polymerization was initiated at 10°C by adding 2 mM $MgSO_4$ (final), where a small magnetic bar in the cell was used for quick mixing. Dilution by 2% of actin and chromaffin granules on addition of $MgSO_4$ was ignored.

DLS measurements

General background information about the DLS method is found in standard textbooks (33, 34). An (8 by N)-bit digital correlator (K7032CE; Malvern Instruments, Malvern, UK) was used to measure the intensity autocorrelation function of the scattered light. A 488-nm beam from an Ar^+ ion laser (model 95; Lexel Corp., Palo Alto, CA) was used as a light source. Details of our spectrometer were described elsewhere (35). The temperature of the scattering cell was controlled at 10 ± 0.05°C. The intensity autocorrelation function $G^2(t)$ is related to the normalized field correlation function $g^1(t)$ of the scattered light by

$$G^2(t) = B\{\beta[g^1(t)]^2 + 1\}, \qquad (1)$$

where $t = mT$ (m = 1, 2, . . . , 128; T, the sampling time), B is the baseline level ($B^{1/2}$ is proportional to the static scattering intensity $\langle I \rangle$, and β is a constant (see Appendix A). For a monodisperse suspension of small particles, we have a simple form of $g^1(t) = \exp(-DK^2t)$, where D is the translational diffusion coefficient of the particle and K is the length of the scattering vector, which equals $(4\pi/\lambda)\sin(\theta/2)$ (λ, the wavelength of light in the medium; θ, the scattering angle). The actual form of $g^1(t)$ of our system is a sum of exponential decays because of a length-distribution of F-actin and presence of granules. Then, the following expansion method is used to obtain a measure of the average decay rate;

$$g^1(t) = [1 + (\mu_2/2)t^2 - (\mu_3/6)t^3]\exp(-\bar{\Gamma}t), \qquad (2)$$

where $\bar{\Gamma}$ is the average value and μ_i is the ith moment around $\bar{\Gamma}$ of the decay rate distribution of $g^1(t)$. The size of B in Eq. 1 is known from data in the monitor channels of the correlator, and four unknowns in Eqs. 1 and 2, i.e., β, $\bar{\Gamma}$, μ_2, and μ_3, can be determined by a least-squares fit. The quantity $\bar{\Gamma}/K^2$ has the same dimension as that of D (cm²/s) and is called an apparent diffusion coefficient, D_{app}. If a simple model is assumed, then D_{app} for a mixture of granules and filaments is given by the weighted average of $D_{app}(*)$'s with respect to the static scattering intensities $I(*)$'s;

$$D_{app} = [D_{app}(f)I(f) + D_{app}(g)I(g)]/\langle I \rangle, \qquad (3)$$

where $\langle I \rangle = I(f) + I(g)$ and $* = f$ and g stand for filament and granule, respectively. For granules in a cage model, $D_{app}(g)$ will be substantially smaller than that for free granules. For more details, see Appendix B.

Throughout this article, we express D_{app} in units of 10^{-9} cm²/s and K^2 in units of 10^{10} cm^{-2}; i.e., $D_{app} = 3$ and $K^2 = 6$, e.g., mean 3×10^{-9} cm²/s and 6×10^{10} cm^{-2}, respectively. We also express $\langle I \rangle$ in an arbitrary but same scale throughout.

Viscosity measurements

The specific viscosity η_{sp} was measured by use of a falling ball viscometer with falling time of 2.2$_7$ s (an average of 10 measurements) for buffer.

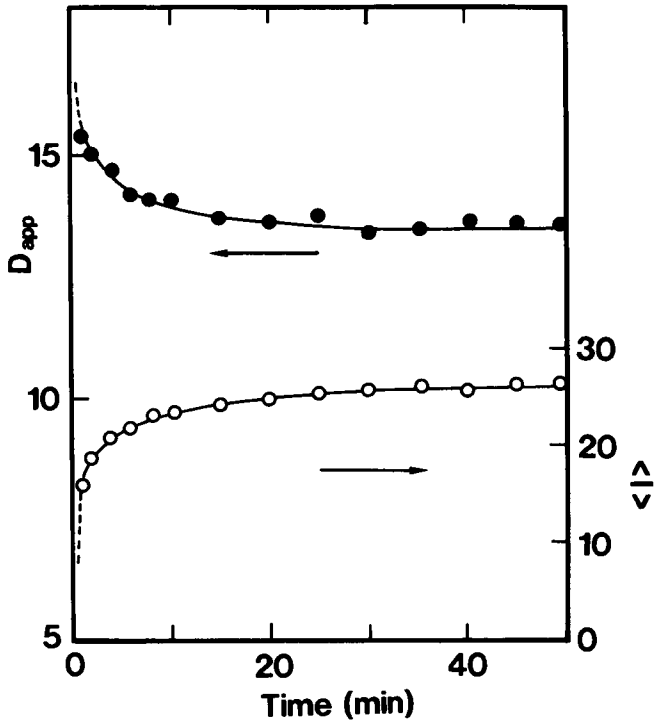

FIGURE 2 Changes in D_{app} and $\langle I \rangle$ after initiation of polymerization of G-actin alone. Data were collected at the scattering angle of 90°.

RESULTS

Actin polymerization

Polymerization of actin alone was first studied. Fig. 2 shows the time courses of the changes in D_{app} and $\langle I \rangle$ at the scattering angle of 90° or $K^2 = 5.86$. In the intensity scale in Fig. 2, $\langle I \rangle = \langle I \rangle_G$ for suspension of G-actin at the present concentration was less than unity. Also D_{app} of G-actin at this condition was ~600. Since polymerization was induced with Mg^{2+} ions, the nucleation process was so fast that we could not observe the very initial stage (i.e., nucleation and early elongation stages) of actin polymerization. Namely, $\langle I \rangle$ was so high and D_{app} was so low compared with those of G-actin even at the first observed point. Then, it is suggested that (*a*) the nucleation and elongation processes finished within the first few minutes and (*b*) the gradual increase in $\langle I \rangle$ and decrease in D_{app} with time in Fig. 2 were mainly due to size redistribution and partly due to further elongation of filaments.

The above suspension was left standing for >10 h at 4°C, and then the D_{app} vs. K^2 relationship was measured (Fig. 3). This D_{app} vs. K^2 relationship is quite compatible with the previous results on F-actin with the number-average length of 600–800 nm for actin preparation without a column chromatography step (36). The D_{app} vs. K^2 relationship for granules alone is also shown in Fig. 3 for a comparison. The slight wiggling behavior of

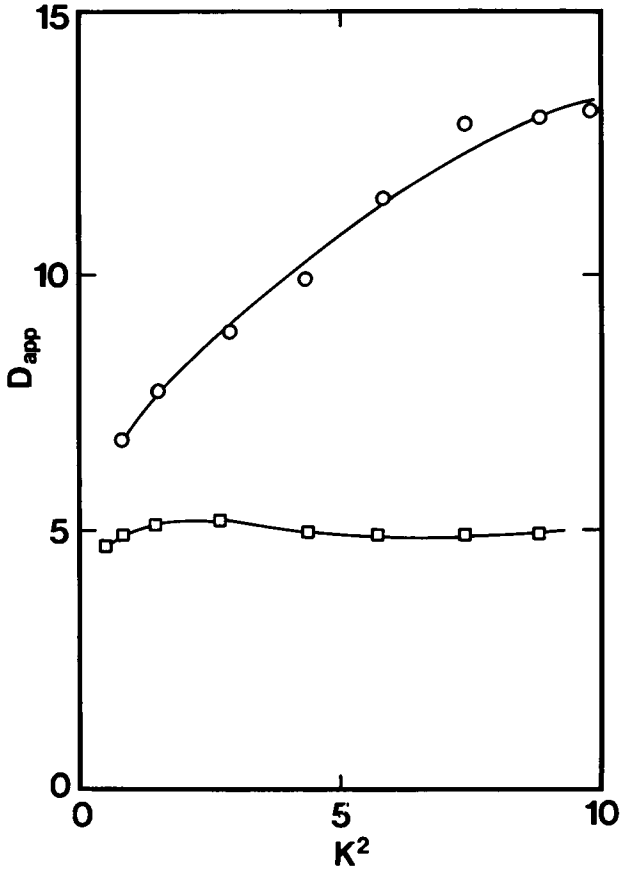

FIGURE 3 The D_{app} vs. K^2 relationships. (○) F-actin alone; the sample in Fig. 1 was left standing at 4°C for >10 h and then examined at 10°C. (□) Chromaffin granules alone (for comparison).

D_{app} against K^2 for granules has been analyzed quantitatively elsewhere (37).

Actin polymerization in the presence of chromaffin granules

Polymerization of actin in the presence of chromaffin granules was studied. Fig. 4 shows the first 20-min portions of the time courses of changes in D_{app} and $\langle I \rangle$ at the scattering angle of 90°. (Although not measured in this study, D_{app} might start from 5, the value for granules alone in Fig. 3, and $\langle I \rangle$ from $I(g)$ because of a very weak contribution to $\langle I \rangle$ from G-actin at time 0.) As is expected, no appreciable effect of free Ca^{2+} ions was observed on these time courses. As for a very slight increase in $\langle I \rangle$ with time, there are at least two possibilities: one is that a large and steady contribution to $\langle I \rangle$ ($=I(f) + I(g)$) from $I(g)$ of granules smeared a change in $I(f)$ due to elongation of filaments with time and another may be that the granules (α-actinin molecules on the surface of a granule) facilitated nucleation for polymerization of actin as observed by electron microscopy (6), so that the elongation finished very soon after initiation of polymerization. For the present system of a mixture of actin filaments and chromaffin granules, the D_{app} value will be given by Eq. 3. Then, from Figs. 2 and 4, it is observed that (*a*) the size redistribution with time of filaments more drastically decreased the D_{app} value in Fig. 4 than in Fig. 2, leading to a prediction that chromaffin granules were confined in cages formed by actin filaments, and (*b*) the D_{app} value in Fig. 4 rapidly became smaller than 5 for granules alone, leading to another prediction that the motion of granules in cages was strongly restricted. By the method described in Appendix B, the size of $D_{app}(g)$ can be estimated as shown by squares in Fig. 4. (The change in $D_{app}(g)$ with time is virtually the same as that in D of PLS previously observed (26).)

The above suspensions were left standing for 24 h at 4°C, and then the D_{app} vs. K^2 relationships were mea-

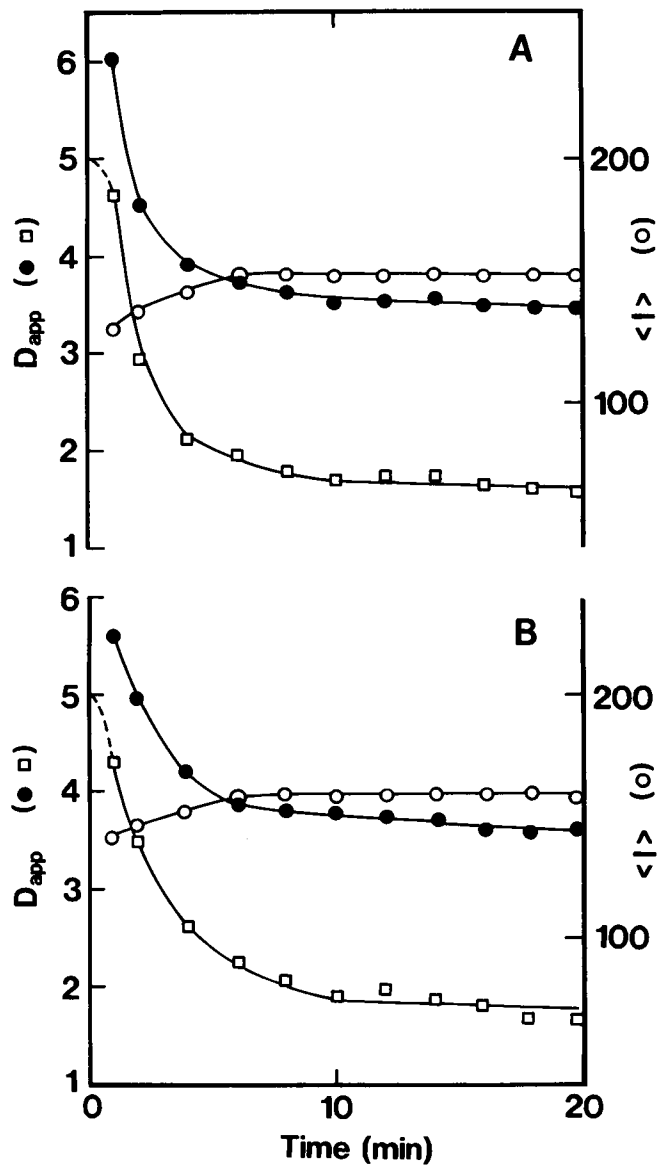

FIGURE 4 Changes in D_{app} (●) and $\langle I \rangle$ (○) after initiation of polymerization of G-actin in the presence of chromaffin granules. (*A*) pCa > 7 and (*B*) pCa = 5. Data were collected at the scattering angle of 90°. (□) The estimated size of $D_{app}(g)$ at 90° (see Appendix B).

sured (Fig. 5). The absolute size and K^2 dependence of D_{app} were essentially the same, both in the presence and absence of 10 μM free Ca^{2+} ions. Since $D_{app}(g)$ would behave virtually flat against K^2 also for granules confined in cages, the K^2 dependence of D_{app} in Fig. 5 came solely from the K^2-dependence of $I(f)/I(g)$ in Eq. 3 and K^2 dependence of $D_{app}(f)$ (something like D_{app} for F-actin alone in Fig. 3). Smaller values of D_{app} than 5 suggest that in the equilibrium state after size redistribution, a network was formed by entanglement of actin filaments, and chromaffin granules were confined in the cages. By the method described in Appendix B, the $D_{app}(g)$ vs. K^2 relationship also can be obtained as shown by squares in Fig. 5.

Effect of gelsolin on actin network preformed in the presence of chromaffin granules

Polymerization of actin in the presence of granules was first carried out, and the F-actin/granule suspensions were incubated for 24 h at 4°C. Then, 0.19 mg/ml gelsolin (final) was added to the above suspensions under a mild stirring in the light-scattering cell (the molar ratio of actin monomers to gelsolin of 10). The consecutive measurement of the DLS spectrum at the scattering angle of 90° was made immediately after mild stirring for 30 s. At pCa > 7 (Fig. 6 *A*), no appreciable change in D_{app} took place. In the $\langle I \rangle$ versus time relationship, a small increase followed by a small decrease was observed. This change in $\langle I \rangle$ may or may not be important, but we ignore it in what follows. (The initial large drop in $\langle I \rangle$ was due to dilution of actin filaments and chromaffin granules on addition of gelsolin; see Fig. 6.) At pCa = 5 (Fig. 6 *B*), on the other hand, a rapid and large increase in D_{app} took place in a first few minutes, which was then followed by a gradual increase. At this pCa, however, $\langle I \rangle$ slightly decreased with time. The severing function of gelsolin in the presence of 10 μM free Ca^{2+} ions is responsible for the large increase in D_{app}, because for this mixture, a value of D_{app} larger than 5 (the size for granules alone) could result only when a substantial number of granules became free due to disappearance of cages formed by actin filaments. Severing of long filaments results in larger $D_{app}(f)$ and $D_{app}(g)$ in

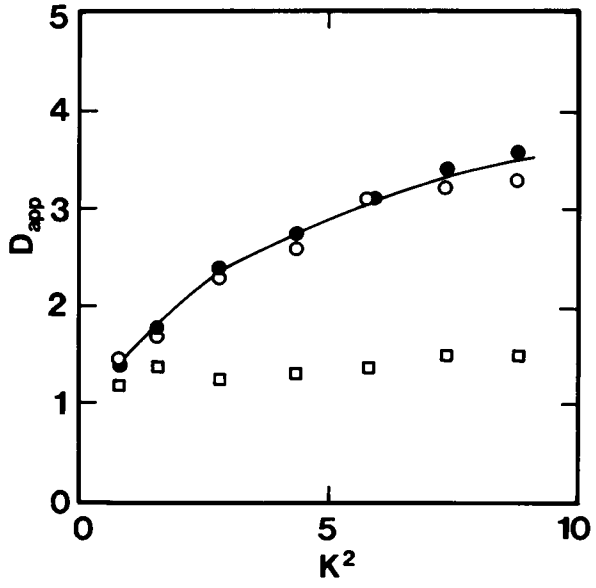

FIGURE 5 The D_{app} vs. K^2 relationships. (○) pCa > 7; (●) pCa = 5. The samples in Fig. 4 were left standing at 4°C for 24 h and then examined at 10°C. (□) The estimated size of $D_{app}(g)$ (see Appendix B).

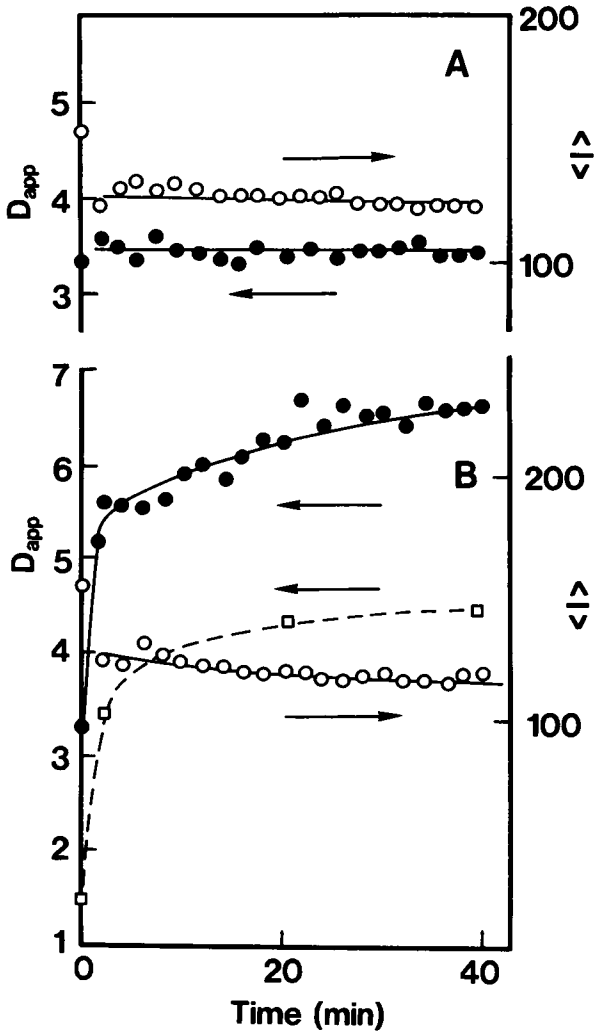

FIGURE 6 Changes in D_{app} (●) and $\langle I \rangle$ (○) after addition of gelsolin to a mixture of F-actin and chromaffin granules. (*A*) pCa > 7 and (*B*) pCa = 5. After the addition of 0.19 mg/ml gelsolin (final) to samples similar to those in Fig. 5, data were collected at the scattering angle of 90° (but, those at time 0 were taken from Fig. 5). Large drops in $\langle I \rangle$'s in *A* and *B* just after the addition of gelsolin were due to dilution of F-actin and chromaffin granules; the final concentration of chromaffin granules was 0.40$_5$ mg/ml and that of F-actin was 0.81 mg/ml (the molar ratio of actin monomers to gelsolin of 10). (□) The estimated size of $D_{app}(g)$ at 90° (see Appendix C).

Eq. 3. By the method described in Appendix C, the sizes of $D_{app}(f)$ and $D_{app}(g)$ can be estimated, and $D_{app}(g)$ is shown by squares in Fig. 6 *B*.

It is well known that the length distribution of in vitro reconstituted F-actin is of an exponential type at the equilibrium state (38). It is not clear whether or not the length distribution is also exponential for F-actin polymerized in the presence of granules. In any case, at a time when each of longer filaments in the distribution is severed into two (to three) pieces, the cages formed by entanglement of long filaments virtually disappear. However, in the time range in Fig. 6, filaments are, on the average, still long enough for them to contribute to D_{app} of the mixture, because D_{app} is larger than 5 (the size of granules alone). As time goes on, free gelsolin molecules, if they still exist, further sever filaments into short pieces and remain bound to the barbed ends of these fragments. It is then expected that (*a*) actin monomers dissociate from the pointed ends of these fragments; (*b*) actin monomers thus produced can bind to the barbed ends of uncapped fragments and/or form nuclei for polymerization; and (*c*) as a result of these processes, the size redistribution will proceed to some extent with a very low rate.

The above suspensions were left standing for 24 h at 4°C, and then the D_{app} vs. K^2 relationships were measured (Fig. 7). At pCa > 7, the absolute values and K^2 dependence of D_{app} are quite the same as those in Fig. 5, suggesting no effect of gelsolin on actin filaments at all. At pCa = 5, on the other hand, the D_{app} vs. K^2 relationship at the equilibrium state is distinctly different from that at pCa > 7 and those in Fig. 5. The fact that D_{app} values at low K^2's are smaller than 5 suggests either most granules undergo a little restricted Brownian motion or some fractions of them are still confined in cages. In any case, motional freedom of granules is concluded to substantially increase as a result of severing action of gelsolin in the presence of free Ca^{2+} ions.

Additional measurements

After the analysis described in Appendixes B and C had been completed, we were aware of the following points. At the molar ratio of actin monomers to gelsolin of 10, G-actin is expected to polymerize into short F-actin with a length of, say, 50 nm on the average. If the preformed F-actin were severed into fragments with this length, then $I(f)$ would be so small that $\langle I \rangle$ would be close to $I(g)$. But this was not the case, because $I(f):I(g)$ decreased from 1:5 to 1:7 (Fig. 6 *B*) and D_{app}'s at $K^2 > 2.5$ were larger than 5 (Fig. 6 *B* and filled circles in Fig. 7). Although the analysis in Appendix C may not be very accurate, it indeed suggested that the preformed F-actin was severed into two to three pieces on the average. Then, we examined this difference by measuring the specific viscosity, η_{sp}, as a quick and intuitive reference. In this viscometry was used a gelsolin preparation different

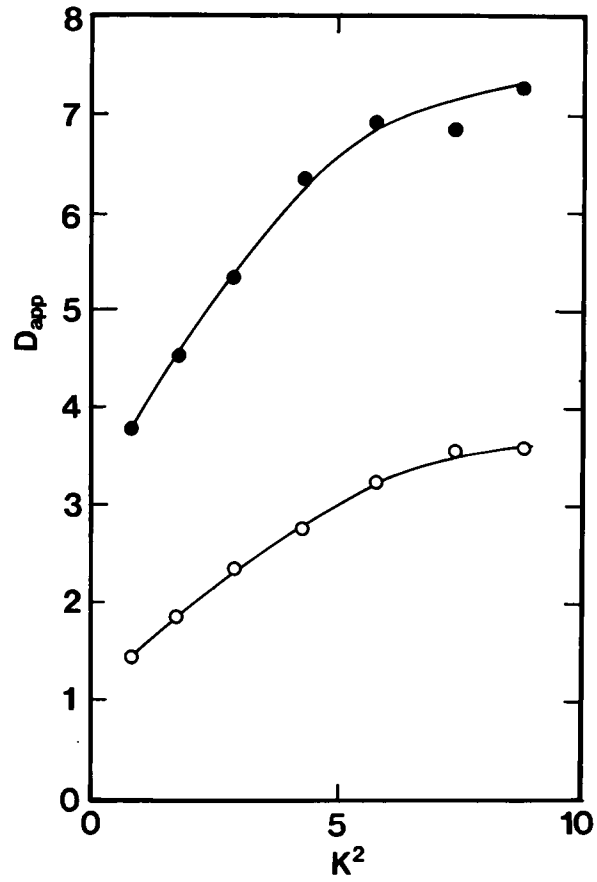

FIGURE 7 The D_{app} vs. K^2 relationships. (○) pCa > 7; (●) pCa = 5. The samples in Fig. 6 were left standing at 4°C for 24 h and then examined at 10°C.

from that used in the above DLS, because almost 3 yr had passed between these two measurements.

Fig. 8 shows some of the η_{sp} versus time relationships. Irrespective of the presence (*filled symbols*) and absence (*open symbols*) of chromaffin granules, it is clearly seen that (*a*) a viscosity increase in the polymerization phase of G-actin was smaller in the presence of gelsolin (*triangles*) than in its absence (*circles*), (*b*) a large viscosity drop was observed just after the addition of gelsolin to the preformed network of F-actin (*circles* in the depolymerization phase), and (*c*) the falling-off level of viscosity at pCa = 5 in the depolymerization phase (*circles*) was twice or more larger than the final level of viscosity in the polymerization phase of G-actin in the presence of gelsolin (*triangles*). The observations very similar to the above ones (without chromaffin granules) have been reported for solvent components of 2 mM $MgCl_2$ and 100 mM KCl instead of 2 mM $MgSO_4$ in our case (39). The first two observations proved a high activity of gelsolin. The third observation suggested again that the average length of F-actin severed by gelsolin was substantially longer than the average length of F-actin polymerized in the presence of gelsolin.

Other observations to be noted in Fig. 8 are as follows. One is that the initial values of 0.60 (*top arrow*) and 0.43

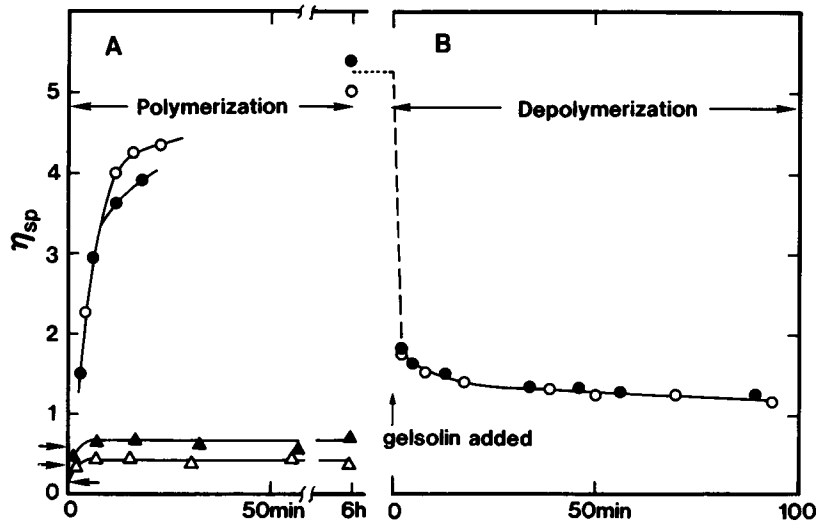

FIGURE 8 The η_{sp} versus time relationships. (*A*) Polymerization phase in the absence (*circles*) and presence (*triangles*) of gelsolin: (○) 0.5 mg/ml G-actin, (●) 0.5 mg/ml G-actin and 0.5 mg/ml chromaffin granules, (△) 0.5 mg/ml G-actin and 0.1 mg/ml gelsolin, and (▲) 0.5 mg/ml G-actin, 0.5 mg/ml, chromaffin granules, and 0.1 mg/ml gelsolin were polymerized at 20°C and pCa = 5 in 300 mM sucrose, 10 mM MOPS, pH 7.0, 0.2 mM MgATP, 0.1 mM PMSF, and 2 mM $MgSO_4$. The molar ratio of actin monomers to gelsolin was 11 in △, ▲. The initial η_{sp} values were measured in the absence of $MgSO_4$; the top arrow indicates the initial value for ●, the middle for ▲, and the bottom for ○, △. (*B*) Depolymerization phase in the absence (○) and presence (●) of chromaffin granules at pCa = 5. On addition of 0.09 mg/ml gelsolin (final) to the above solutions (○, ● in *A*), F-actin and chromaffin granules were diluted to 0.4 mg/ml, and the molar ratio of actin monomers to gelsolin was 10.

(*middle arrow*) were, respectively, three and two times larger than the sum of 0.13 (*bottom arrow*) and 0.08 for 0.5 mg/ml chromaffin granules alone. This observation probably suggests, even in the absence of 2 mM $MgSO_4$, formation of very short F-actin due to nucleation facilitated by α-actinin on the surface of granules. The other is that the final value of viscosity was larger in the presence of chromaffin granules (*filled triangle*) than in its absence (*open triangle*). These two observations may suggest that the situation in our model system was in part similar to that in Fig. 1 *a*. This possibility has to be taken into account in quantitative evaluation of the present results, because we derived Eq. 4, and hence Eqs. 3 and 5, by assuming no direct binding between chromaffin granules and F-actin as in Fig. 1 *c*. (The absolute size of viscosity, especially at high viscosity regions, was very sensitive to experimental conditions. This is a reason why the viscosity for F-actin alone at an intermediate time range was higher than that for F-actin/granules in this particular case.)

As to the third observation, we first considered it to be due to no addition of KCl to our preparation on actin polymerization. It was found, however, that irrespective of the presence and absence of Cl^-, K^+, and/or sucrose, the falling-off levels of viscosity strongly depended on the degree of mechanical perturbation (mixing) on addition of gelsolin to the preformed network of actin filaments. Under mild mixing of the suspension by sucking up and down two to three times with a pipette whose tip had been cut to widen it greatly, was obtained the η_{sp} versus time relationships as shown in Fig. 8. On the other hand, under vigorous mixing by sucking up and down more than five times with the pipette whose tip had not been cut, the falling-off levels of η_{sp} were almost close to the final values (*triangles*) in the polymerization phase. The falling-off levels of η_{sp} at the molar ratio of actin monomers to gelsolin of 10 under mild mixing (as in DLS measurements) were equal to the final values in the polymerization phase at the molar ratio around 100. This result was consistent with the DLS result analyzed in Appendix C. These findings strongly suggested a difference in capping and severing activities of gelsolin. We inferred that gelsolin molecules reduced the actin–actin bond strength at their attached points on F-actin to a great extent. The actin filaments with such weakened bonds would be fragmented by thermal agitation if they were long (fluctuation-induced severing) and also by mechanical perturbation even if they were short (applied force-induced severing). In any case, the barbed ends of fragments were immediately capped by gelsolin, resulting in a drop in η_{sp} depending on mixing conditions. It should be noted that the gelsolin we used indeed severed F-actin without any mechanical perturbation; I-bands disappeared when myofibrils were bathed in Ca-rigor solution containing gelsolin (31).

DISCUSSION

The secretory cell accepts an external chemical signal by receptor molecules on the cell surface. Through intervention of various molecular processes by second messengers, the free Ca^{2+} ion concentration in the cytosol finally increases from a submicromolar resting level to a micromolar activated one (19). The molecular mecha-

nism of signal transduction in the first stage has been studied extensively in the past several years (40, 41). However, few studies have been made for the final stage to exocytosis (42). Based on the present results and several pieces of evidence in the literature, we propose a molecular model of this final step.

Electron microscopic observations for macrophages and platelets showed that a large amount of gelsolin molecules resides in 80–100-nm cortical zones and on the cell membrane (21, 22). A large amount of gelsolin molecules must also exist in diffusible and/or bound states everywhere in cytoplasm of many mammalian cells. Electron microscopic observations by use of a quick-freeze method showed that highly dense actin filaments extend from protein molecules on the inner surface of the plasma membrane. By means of immunoelectron microscopy, these proteins are identified as gelsolin, each of which binds to a cluster of phosphatidylinositol 4,5-bisphosphate (PIP_2) (22).

In a static state, secretory granules are held in the actin network at least in three ways (Fig. 1). In the 80–100-nm peripheral region, which is a three times thinner layer than the diameter of granules, highly dense actin network prevents secretory granules from directly touching the cell membrane (6). As a prelude of exocytosis, this actin network must dissociate or loosen for granules to contact freely with fusion sites on the membrane (2). As has been generally assumed and partly confirmed experimentally (e.g., review references 9 and 17), we also assume a series of the following steps: (*a*) activation of actin-severing proteins, e.g., gelsolin, by free Ca^{2+} ions (at a micromolar level) for disassembly of actin network; (*b*) free, or slightly restricted, diffusion of a granule to a fusion site on the membrane; (*c*) fusion with cell membrane and release of the content of the granule; and (*d*) revesiculation from the fused membrane and reformation of actin network. We introduce a biophysical model for rearrangement of the actin network before and after exocytosis. In our simple model, the movement of granules at the resting state ($pCa > 7$) is restricted in cages formed by actin filaments (situation 1). Before exocytosis, these actin filaments are disassembled by gelsolin at $pCa \leq 6$ (situation 2). After an exocytotic event, the free Ca^{2+} ion concentration returns to the resting one ($pCa > 7$). Then, actin filaments are reformed in the peripheral region (situation 3). Subsequent size redistribution of filaments results in formation of cages that confine granules in them (going back to situation 1). This study concerned only situations 1 and 2.

The present results (Figs. 4 and 5) suggested a very restricted motion of granules in cages formed by actin filaments. In the present in vitro system, the cages are temporary, because they are ceaselessly created and annihilated as a result of almost free translation of filaments along their long axis. Thus, granules can travel over any distance with a very low mobility. As shown in Fig. 1, however, many filaments in an intact cell are anchored on the cell membrane (22), so that the cages formed by these filaments are permanent in the resting state. Thus, granules are confined literally in these permanent cages. This supports situation 1. As suggested (Fig. 6 *B*), gelsolin molecules ($+Ca^{2+}$) immediately fragmented actin filaments into short pieces and remained bound to the barbed ends of these actin fragments. The present results (Figs. 6 *B* and 7) suggested a substantial increase in motional freedom of granules. This supports situation 2. Simultaneously, actin filaments may disappear from the special area of a fusion site. In an intact cell, various actin-severing proteins may coexist with gelsolin, one of which is scinderin (13), and they will work to speed up the disassembly process of actin filaments in vivo. We did not study, by the DLS method, the polymerization process of G-actin in the presence of gelsolin. However, there are several studies that suggest formation of short pieces of actin filaments even in the presence of gelsolin and Ca^{2+} ions (15, 39, 43) (see also triangles in Fig. 8). These support situation 3. A gelsolin molecule bound to the barbed end of an actin fragment does not dissociate spontaneously even at $pCa > 7$ (44). In an intact cell, the cell membrane contains many PIP_2 molecules that may liberate gelsolin molecules from fragments of actin filaments (44–46), resulting in a rapid elongation and size redistribution of actin filaments by "annealing" (36) or a rapid reformation of cages that confine granules (going back to situation 1). In addition to PIP_2, various molecules not considered here (and not identified yet) would work to speed up the reassembly process of actin filaments in vivo.

In addition, in situation 2, some fusion proteins and phospholipases might be activated by free Ca^{2+} ions, and they might be involved in the process of membrane fusion. But, so far there is no evidence that the aid of these proteins is indispensable for membrane fusion. Rather, a change in the physical state of a granule membrane seems to be important for initiation of membrane fusion. The elasticity of the granule membrane has been found to decrease sharply and greatly at around $pCa = 6$ (23, 24). The flexibility of the granule membrane is necessary for the granule to touch the cell membrane with some size of area (and not a point contact).

To mimic a cytosolic situation as closely as possible, high concentrations of actin and granules were adopted at the expense of quality of DLS measurements to some extent. Although multiple scattering may be serious at low angles, we did not examine it quantitatively and assumed it to be negligible at the angle of 90° (Figs. 2, 4, and 6). Although $G^2(t)$ decayed smoothly, the third-order expansion, Eq. 2, gave very large Q values (see Fig. 10). In addition to these, the length distribution of in vitro reconstituted F-actin is very broad. Due to these facts, quite a quantitative analysis of DLS results is not possible. In the Appendixes below, some semiquantita-

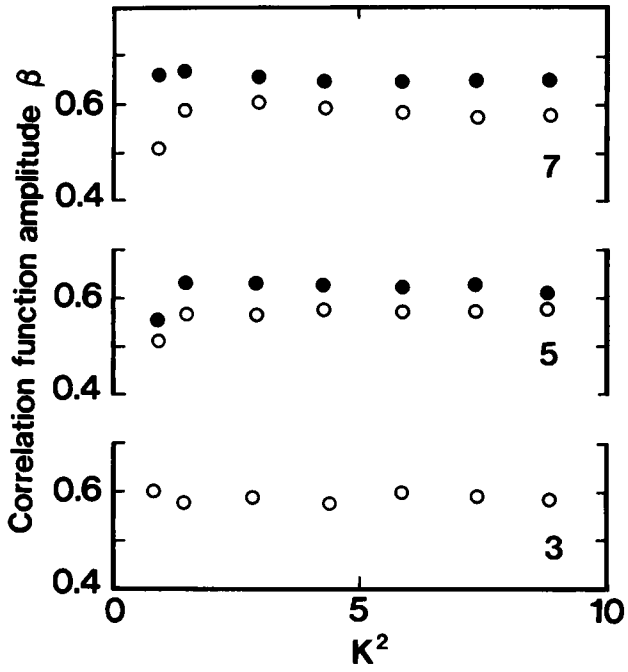

FIGURE 9 The β vs. K^2 relationships. The labels (*3*, *5*, and *7*) correspond to the figure numbers and the symbols to those therein.

tive analyses are made to complement the statements in the text.

APPENDIX A

Correlation function amplitude

The correlation function amplitude, β in Eq. 1, is a measure of how freely the particle diffuses over a probing distance $1/K$. In other words, if the β value becomes small at a given K^2, the particle is trapped on the distance scale of $1/K$. In our optical setup, a dilute suspension of freely diffusing particles gave the β value of ~0.65. The β vs. K^2 relationships (labels *5* and *7* in Fig. 9) suggest that chromaffin granules in the actin network diffuse almost freely over $1/K = 110$ nm even at the lowest K^2 (at the scattering angle of 30°) or a cage diameter is larger than 500 nm (the sum of $1/K$ and the diameter of the granule). Since, however, the β value at the lowest K^2 shows a tendency to become small, the average cage diameter may not be so much larger than 500 nm.

APPENDIX B

Apparent diffusion coefficient

The apparent diffusion coefficient, $D_{app} = \bar{\Gamma}/K^2$, is a measure of how quickly a particle undergoes the Brownian motion. Qualitatively speaking, the larger the D_{app} value is, the larger the mobility is. The decrease in D_{app} with time for actin alone (Fig. 2) is due to elongation/size redistribution of F-actin (36). For long and semiflexible filaments such as F-actin, however, D_{app} increases with K^2 (Fig. 3). This is due to the increasing contribution from rotational and segmental (bending) motions of filaments (47). A little wiggling behavior of the D_{app} vs. K^2 relationship for chromaffin granules alone (Fig. 3) is due to another reason detailed elsewhere (37) and can be ignored in the present examination. Then, the interpretation of a large K^2 dependence of D_{app} in Figs. 5 and 7 is a little complicated.

Although the specific viscosity (see arrows and triangles in Fig. 8) was indeed affected by the presence of granules, DLS results studied so far did not give clear evidence of direct binding between filaments and granules: if there were many filaments extending from α-actinin molecules on the granule membrane as in Fig. 1 *a*, then the scattering intensity $\langle I \rangle$ of the mixture of granules and filaments would be substantially higher than the simple sum of the intensities for filaments alone, $I(f)$, and granules alone, $I(g)$, at the same concentrations as components of the mixture. However, a relation $\langle I \rangle = I(f) + I(g)$ was valid within experimental errors. Furthermore, if the direct binding were appreciable, the β values would be substantially smaller than that for freely diffusing particles. This was not the case (see Appendix A). These lead to a conclusion of no appreciable direct binding between filaments and granules. (A possible effect of granules on the specific viscosity was observed only before the addition of 2 mM $MgSO_4$ and/or during the polymerization phase in the presence of gelsolin, i.e., when viscosity was low. If measurements were made for such situations, then presence of granules might also affect the DLS spectra. In the present experimental conditions, a contribution to DLS spectra from minor filaments extending from granules would be masked by a contribution from major filaments free from binding.) If we assume no direct-binding, then we have (cf. Eq. 2)

$$\langle I \rangle g^1(t) = \sum I(*)[1 + (\mu_2(*)/2)t^2 - (\mu_3(*)/6)t^3] \times \exp[-D_{app}(*)K^2 t], \quad (4)$$

where Σ stands for the sum over $* = f$ and g and notations are the same as those in the text. The first time derivative of Eq. 4 at $t = 0$ gives the average decay rate $\bar{\Gamma}$ of $g^1(t)$ for the mixture, which can be written as in Eq. 3 in the text.

For $D_{app}(f) = D_{app}$ and $I(f) = \langle I \rangle$ in Fig. 2 and D_{app} and $I(g) + I(f) = \langle I \rangle$ in Fig. 4, Eq. 3 gives the $D_{app}(g)$ versus time relationships at 90° as shown by squares in Fig. 4. A rapid decrease of $D_{app}(g)$ suggests a rapid formation of cages by entanglement of long filaments. The same analysis is possible for data in Fig. 5. At the scattering angle of 90°, $I(f) = 26$ is obtained from $\langle I \rangle$ in Fig. 2 and $I(f) + I(g) = 155$ from $\langle I \rangle$ in Fig. 4 (or $I(g) = 129$). These observed values give $I(f)/I(g) = 0.20$, which may be slightly smaller than that at the equilibrium state. At the same angle, we have $D_{app}(f) = 11.4$ from Fig. 3 and $D_{app} = 3.1$ from Fig. 5. Then, Eq. 3 gives $D_{app}(g) = 1.4$ at 90°, which is a little smaller than 1.6–1.7 at time 20 min in Fig. 4. For $D_{app}(f)$ from Fig. 3, D_{app} from Fig. 5, $I(g)$ from Fig. 6 in reference 37, and $I(f)$ from a separate measurement (and scaled as $I(f)/I(g) = 0.20$ at 90°), Eq. 3 gives the $D_{app}(g)$ vs. K^2 relationship as shown by squares in Fig. 5. (This analysis is valid also for open circles in Fig. 7.) The sizes of $D_{app}(g) = 1.2$–1.5 over the present range of K^2 support our interpretation in the text that the granules are confined in cages formed by filaments.

As for $D_{app}(f)$ in a mixture of granules and filaments, D_{app} of F-actin alone with empty cages was assumed. This assumption may or may not be true. Since, however, occupation of cages by granules may reduce only the $D_{app}(f)$ value to some extent, leaving $I(f)$ almost unchanged, the above analysis is still valid semiquantitatively in such a situation. Under such conditions as that, the scattering intensity from PLS was very much higher than that from F-actin; DLS measurements for PLS with diameters 350–400 nm in F-actin solutions gave $D/D_0 = 0.2$–0.3 at 1 mg/ml actin, where D_0 denotes the D value at 0 actin (26). Then, we have $D = 1.0$–1.5 for $D_0 = 5$ (the free value for chromaffin granules). An agreement of this D with the above estimated $D_{app}(g)$ supports the present analysis by use of Eq. 3. Unfortunately, the same analysis as above cannot be applied to the results in Fig. 6 *B*, because we did not study, by the DLS method, the effect of gelsolin on F-actin network preformed in the absence of chromaffin granules. Therefore, an alternative analysis is given below.

APPENDIX C

Polydispersity parameter

From the quantities $\bar{\Gamma}$ and μ_2 in Eq. 2, the so-called polydispersity parameter is defined as $Q = (\mu_2/\bar{\Gamma}^2)$. This Q is a measure of the width

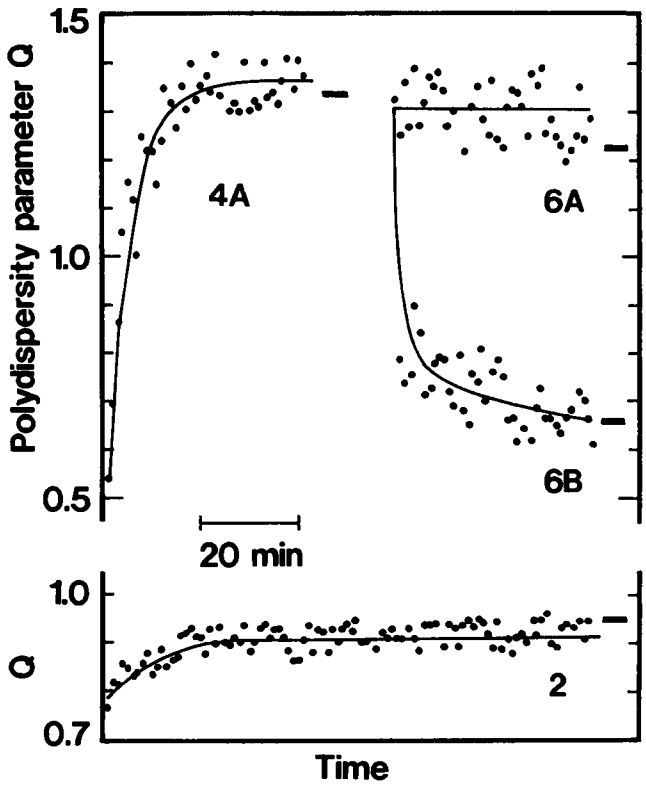

FIGURE 10 The Q versus time relationships. The labels (*2, 4A, 6A,* and *6B*) correspond to the figure numbers, and the thick line segment at the end of each set of data shows the equilibrium Q value.

in the decay rate distribution of $g^1(t)$ around $\bar{\Gamma}$. Fig. 10 depicts Q versus time relationships. The Q value for actin alone (label *2*) was ~0.9 at the plateau. This large Q value is due to very slowly decaying components coming from slow movements of entangled actin filaments. The Q versus time relationship for the mixture of actin and granules at pCa = 5 (data not shown) was almost the same as that with label *4A* at pCa > 7. The Q value (label *4A*) reached 1.3–1.4; this very large Q value is due to a large separation between $D_{app}(f)$ and $D_{app}(g)$ as well as the large Q value of F-actin alone. On addition of gelsolin, this very large Q value quickly decreased to 0.6–0.7 at pCa = 5 (label *6B*), whereas it stayed constant at pCa > 7 (label *6A*); the small Q value at pCa = 5 is mostly due to disappearance of slow movements of entangled filaments as a result of the severing effect of gelsolin.

The second time derivative of Eq. 4 at $t = 0$ gives

$$Q = [D_{app}(f) - D_{app}(g)]^2 I(f)I(g)/[\langle I\rangle D_{app}]^2 + C, \quad (5)$$

where $C = [Q(f)I(f)D_{app}(f)^2 + Q(g)I(g)D_{app}(g)^2]/[\langle I\rangle D_{app}^2]$ and use was made of Eq. 3. The first term on the righthand side of Eq. 5 gives the contribution to Q of the mixture from the separation between $D_{app}(f)$ and $D_{app}(g)$ and the second term, C, from $Q(f)$ and $Q(g)$ of the constituent components. There are four unknowns in Eq. 5, i.e., $D_{app}(*)$ and $Q(*)$ for $* = f$ and g in the mixture. Because we like to know approximate sizes of $D_{app}(f)$ and $D_{app}(g)$, we tentatively put $Q(f) = Q(g) = 0$ or $C = 0$. Then, for given values of Q, D_{app}, and $I(f):I(g) = (\langle I\rangle - I(g)):I(g)$, Eqs. 3 and 5 (with $C = 0$) can give estimates of $D_{app}(f)$ and $D_{app}(g)$.

For $I(f) = 26$ and $I(g) = 129$ (or $I(f):I(g) = 1:5$) at 90° and time 20 min (see Appendix B) and $D_{app} = 3.5$ at time 20 min in Fig. 4 and $Q = 1.4$ in Fig. 10 (label *4A*), Eqs. 3 and 5 give $D_{app}(f) = 12.8$ and $D_{app}(g) = 1.6_5$, which should be compared with the observed value of $D_{app}(f) = 13.5$ in Fig. 2 and the estimated value of $D_{app}(g) = 1.6$–1.7 in Fig. 4. This nice agreement, if not accidental, suggested applicability of Eq. 5 with $C = 0$ to other cases. Then, $g^1(t)$'s were numerically generated for various combinations of $I(*)$, $D_{app}(*)$, $\mu_2(*)$, and $\mu_3(*)$ for $* = f$ and g in Eq. 4, and they were analyzed by the same program as that in the analysis of experimental $G^2(t)$'s. From this simulation, it turned out that the analysis by use of Eqs. 3 and 5 (with $C = 0$) recovered $D_{app}(f)$ and $D_{app}(g)$ with 80% or better accuracy.

In the analysis of data in Fig. 6 *B* by this method, we must assume $I(g) = 129 \times (4/5) = 103$ due to dilution of chromaffin granules. Then, $\langle I\rangle = 118$ at time 40 min gives $I(f) = 15$ or $I(f):I(g) = 1:7$. Then, for $D_{app} = 6.5$ at time 40 min in Fig. 6 *B* and $Q = 0.7$ in Fig. 10 (label *6B*), Eqs. 3 and 5 give $D_{app}(f) = 20.8$ and $D_{app}(g) = 4.4$. Some of estimated $D_{app}(g)$ values are shown by squares in Fig. 6 *B*. Although this analysis may not be very accurate as compared with that in Appendix B, these estimated values for $D_{app}(f)$ and $D_{app}(g)$ are very suggestive. Namely, the estimated value of $D_{app}(f) = 21$ at time 40 min in Fig. 6 *B* is only two times larger than $D_{app}(f) = 11.4$ at 90° (or $K^2 = 5.86$) in Fig. 3. This suggests that longer filaments in the exponential length distribution were severed into two (to three) pieces on the average.

S. Miyamoto and S. Fujime appreciate the support from Mitsubishi Kasei Institute of Life Sciences (Tokyo, Japan), where all the DLS measurements in this study were carried out just before they moved to their present institutions (1989).

Received for publication 11 June 1992 and in final form 16 November 1992.

REFERENCES

1. Cheek, T. R., and R. D. Burgoyne. 1986. Nicotin-evoked disassembly of cortical actin filaments in adrenal chromaffin cells. *FEBS (Fed. Eur. Biochem. Soc.) Lett.* 207:110–114.
2. Burgoyne, R. D., and T. R. Cheek. 1987. Reorganization of peripheral actin filaments as a prelude to exocytosis. *Biosci. Rep.* 7:281–288.
3. Aunis, D., and M.-F. Bader. 1988. The cytoskeleton as a barrier to exocytosis in secretory cells. *J. Exp. Biol.* 139:253–266.
4. Sontag, J. M., D. Aunis, and M. F. Bader. 1988. Peripheral actin filaments control calcium-mediated catecholamine release from streptolysin-O-permeabilized chromaffin cells. *Eur. J. Cell Biol.* 46:316–326.
5. Hirokawa, N., K. Sobue, K. Kanda, A. Harada, and H. Yorifuji. 1989. The cytoskeletal architecture of the presynaptic terminal and molecular structure of synapsin 1. *J. Cell Biol.* 108:111–126.
6. Burgoyne, R. D. 1984. Mechanisms of secretion from adrenal chromaffin cells. *Biochim. Biophys. Acta.* 779:201–216.
7. Pollard, H. B., C. E. Creutz, V. Fowler, J. Scott, and C. J. Pazoles. 1982. Calcium dependent regulation of chromaffin granule movement, membrane contact, and fusion during exocytosis. *Cold Spring Harbor Symp. Quant. Biol.* 46:819–834.
8. Aunis, D., and D. Perrin. 1984. Chromaffin granule membrane-F actin interactions and spectrin-like protein of subcellular organelles: a possible relationship. *J. Neurochem.* 42:1558–1569.
9. Trifaro, J.-M., M.-F. Bader, and J.-P. Doucet. 1985. Chromaffin cell cytoskeleton: its possible role in secretion. *Can. J. Biochem. Cell Biol.* 63:661–679.
10. Bader, M.-F., J.-M. Trifaro, O. K. Langley, D. Thierse, and D. Aunis. 1986. Secretory cell actin-binding proteins: identification of a gelsolin-like protein in chromaffin cells. *J. Cell Biol.* 102:636–646.
11. Maekawa, S., M. Toriyama, S. Hisanaga, N. Yonezawa, E. Endo,

N. Hirokawa, and H. Sakai. 1989. Purification and characterization of a Ca^{2+}-dependent actin filament severing protein from bovine adrenal medullae. *J. Biol. Chem.* 264:7458–7465.

12. Maekawa, S., and H. Sakai. 1990. Inhibition of actin regulatory activity of the 74-kDa protein from bovine adrenal medullae (adseverin) by some phospholipids. *J. Biol. Chem.* 265:10940–10942.
13. Rodriguez Del Castillo, A., S. Lemaire, L. Tchakarov, M. Jeyapragasan, J.-P. Doucet, M. L. Vitale, and J.-M. Trifaro. 1990. Chromaffin cell scinderin, a novel calcium-dependent actin filament-severing protein. *EMBO (Eur. Mol. Biol. Organ.) J.* 9:43–52.
14. Yin, H. L., and T. P. Stossel. 1979. Control of cytoplasmic actin gelsol transformation by gelsolin, a calcium dependent regulatory protein. *Nature (Lond.)* 281:583–586.
15. Yin, H. L., J. H. Hartwig, K. Maruyama, and T. P. Stossel. 1981. Ca^{2+} control of actin filament length. Effect of macrophage gelsolin on actin polymerization. *J. Biol. Chem.* 256:9693–9697.
16. Matsudaira, P., and P. Janmey. 1988. Pieces in the actin severing protein puzzle. *Cell.* 54:139–140.
17. Stossel, T. P. 1989. From signal to pseudopod: how cells control cytoplasmic actin assembly. *J. Biol. Chem.* 264:18261–18264.
18. Vitale, M. L., A. Rodriguez Del Castillo, L. Tchakarov, and J.-M. Trifaro. 1991. Cortical filamentous actin disassembly and scinderin redistribution during chromaffin cell stimulation precede exocytosis, a phenomenon not exhibited by gelsolin. *J. Cell Biol.* 113:1057–1067.
19. Cheek, T. R., T. R. Jackson, A. J. O'Sullivan, R. B. Moreton, M. J. Berridge, and R. D. Burgoyne. 1989. Simultaneous measurements of cytosolic calcium and secretion in single bovine adrenal chromaffin cells by fluorescence imaging of fura-2 in cultured cells. *J. Cell Biol.* 109:1219–1227.
20. O'Sullivan, A. J., T. R. Cheek, R. B. Moreton, M. J. Berridge, and R. D. Burgoyne. 1989. Localization and heterogeneity of agonist-induced changes in cytosolic calcium concentration in single bovine adrenal chromaffin cells from video imaging of fura-2. *EMBO (Eur. Mol. Biol. Organ.) J.* 8:401–411.
21. Cooper, J. A., D. J. Loftus, C. Frieden, J. Bryan, and E. L. Elson. 1988. Localization and mobility of gelsolin in cells. *J. Cell Biol.* 106:1229–1240.
22. Hartwig, J. H., K. A. Chambers, and T. P. Stossel. 1989. Association of gelsolin with actin filaments and cell membranes of macrophages and platelets. *J. Cell Biol.* 108:467–479.
23. Miyamoto, S., and S. Fujime. 1988. Regulation by Ca^{2+} of membrane elasticity of bovine chromaffin granules. *FEBS (Fed. Eur. Biochem. Soc.) Lett.* 238:67–70.
24. Miyamoto, S., and S. Fujime. 1990. Elastic behavior of zymogen granule membranes in response to changes in pH and pCa. *Biophys. J.* 57:615–619.
25. Miyamoto, S., T. Maeda, and S. Fujime. 1988. Change in membrane elastic modulus on activation of glucose transport system of brush border membrane vesicles studied by osmotic swelling and dynamic light scattering. *Biophys. J.* 53:505–512.
26. Newman, J., N. Mroczka, and K. L. Schick. 1989. Dynamic light scattering measurements of the diffusion of probes in filamentous actin solutions. *Biopolymers.* 28:655–666.
27. Newman, J., G. Gukelberger, K. L. Schick, and K. S. Zener. 1991. Probe diffusion in solutions of filamentous actin formed in the presence of gelsolin. *Biopolymers.* 31:1265–1271.
28. Straub, F. B. 1943. Actin. *Studies Inst. Med. Chem. Univ. Szeged.* 2:3–15.
29. Ebashi, S., and K. Maruyama. 1965. Preparation and some properties of α-actinin-free actin. *J. Biochem. (Tokyo).* 58:20–26.
30. Spudich, J. A., and S. J. Watt. 1971. The regulation of rabbit skeletal muscle contraction. 1. Biochemical studies of the interaction of the tropomyosin-troponin complex with actin and the proteolytic fragments of myosin. *J. Biol. Chem.* 246:4866–4871.
31. Funatsu, T., H. Higuchi, and S. Ishiwata. 1990. Elastic filaments in skeletal muscle revealed by selective removal of thin filaments with plasma gelsolin. *J. Cell. Biol.* 110:53–62.
32. Kwiatkowski, D. J., T. P. Stossel, S. H. Orkin, J. E. Mole, H. R. Colten, and H. L. Yin. 1986. Plasma and cytoplasmic gelsolins are encoded by a single gene and contain a duplicated actin-binding domain. *Nature (Lond.).* 323:455–458.
33. Chu, B. 1974. Laser Light Scattering. Academic Press Inc., New York. 317 pp.
34. Berne, B., and R. Pecora. 1975. Dynamic Light Scattering. Interscience, New York. 376 pp.
35. Fujime, S., S. Ishiwata, and T. Maeda. 1984. Dynamic light scattering study of muscle F-actin. *Biophys. Chem.* 20:1–20.
36. Masai, J., S. Ishiwata, and S. Fujime. 1986. Dynamic light scattering study on polymerization process of muscle actin. *Biophys. Chem.* 25:253–269.
37. Fujime, S., M. Takasaki-Ohsita, and S. Miyamoto. 1988. Dynamic light scattering from polydisperse suspensions of large spheres. Characterization of isolated secretory granules. *Biophys. J.* 54:1179–1184.
38. Oosawa, F., and S. Asakura. 1975. Thermodynamics of the Polymerization of Proteins. Academic Press Inc., London/New York/San Francisco. 204 pp.
39. Porte, F., and M.-C. Harricane. 1986. Interaction of plasma gelsolin with actin. Isolation and characterization of binary and ternary plasma-gelsolin-actin complexes. *Eur. J. Biochem.* 154:87–93.
40. Gilman, A. G. 1987. G-proteins: transducers of recepter-generated signals. *Annu. Rev. Biochem.* 56:615–649.
41. Berridge, M. J., and R. F. Irvine. 1989. Inositol phosphates and cell signaling. *Nature (Lond.).* 341:197–205.
42. De Camilli, P., and R. Jahn. 1990. Pathways to regulated exocytosis in neurons. *Annu. Rev. Physiol.* 52:625–645.
43. Janmey, P. A., J. Peetermans, K. S. Zaner, T. P. Stossel, and T. Tanaka. 1986. Structure and mobility of actin filaments as measured by quasielastic light scattering, viscometry and electron microscopy. *J. Biol. Chem.* 261:8357–8362.
44. Janmey, P. A., and T. P. Stossel. 1987. Modulation of gelsolin function by phosphatidylinositol 4,5-bisphosphate. *Nature (Lond.)* 325:362–364.
45. Janmey, P. A., and P. T. Matsudaira. 1988. Functional composition of villin and gelsolin. (Effects of Ca^{2+}, KCl and polyphosphoinositides). *J. Biol. Chem.* 236:16738–16743.
46. Yin, H. L., K. Iida, and P. A. Janmey. 1988. Identification of a polyphosphoinositide-modulated domain in gelsolin which binds to the sides of actin filaments. *J. Cell Biol.* 106:805–812.
47. Fujime, S., M. Takasaki-Ohsita, and S. Ishiwata. 1987. Dynamic light scattering study of muscle F-actin II. *Biophys. Chem.* 27:211–224.